# Testing of the sensing element of a capacitive micromechanical accelerometer

**A.V.Styazhkina[1], A.A. Belogurov[2], N.S.Sharagina[2], Ya.V.Belyev[3], N.V. Moiseev[3]**

[1]PhD Student Concern CSRI Elektropribor, JSC, Saint-Petersburg, Russia
[2]Engineer Concern CSRI Elektropribor, JSC
[3]Candidate of Technical Science Concern CSRI Elektropribor, JSC

E-mail: anna_yakimov@mail.ru

**Abstract**. Sensing element is one of the main parts of a micromechanical accelerometer. It determines a lot of parameters of the whole device. Its design flow is a complex process including the steps from the analysis of technical and technological requirements to testing the manufactured devices. Testing is one of the most important steps because it allows not only getting the final characteristics of the chip, but also verifying and specifying the mathematical model of the sensing element for future designs. The paper presents the results of micromechanical accelerometer sensing element testing. Special attention is given to the steps of wafer-level testing and testing with an integrated circuit in the accelerometer.

## Introduction

The area of competence of Concern CSRI Elektropribor, JSC, is navigation, gyroscopy, gravimetry, etc. The base of the designed systems is inertial sensors built on different principles, including microelectromechanical technology [1]. Today the concern has a production of micromechanical accelerometers (MMA) and gyroscopes based on imported integrated circuit (IC). The mechanical part of the gyroscope, the sensing element (SE), was designed in 2000-ies, whereas the MMA SE was purchased. Thus, there are two main goals: to improve the final characteristics of the serial devices, and to design sensors based on our own SE and IC and to localize the production in Russia.

The second task was solved for the MMA. The general results that are presented in [2] describe the whole MMA design flow (Fig. 1), whereas this paper focuses on the test procedure and test results for our MMA SE.

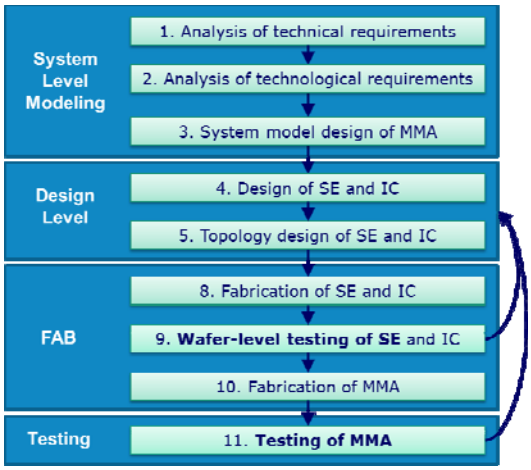


Fig. 1. MMA design flow

Much attention is given to the test procedure, since it is one of the main design flow milestones along with preliminary modeling and joint modeling of SE and IC. Testing at the intermediate production steps such as wafer-level test allows reducing time and cost of the final product by selecting chips with required characteristics. In addition, we can

take into account the wafer-level test results for further design and fabrication iterations. Finally, we use the SE wafer-level test results for preliminary IC trimming.

## 1. Subject of testing and controlled parameters

The subject of testing, a sensing element of the capacitive MMA designed at Concern CSRI Elektropribor, JSC (SE-ELP) [3], can be divided into mechanical and electrical parts. The mechanical part is a frame form mass, suspended on 12 meander-shaped springs (Fig. 2a). The main mechanical parameters are stiffness matrix, resonance frequencies and damping coefficient matrix.

The electrical part consists of four electrode groups, every two of which form a differential electrode structure for self-testing (ES1 and ES2) or for detecting the displacement of the moving part (ED1 and ED2). An electrode group is built on the principle of gap changing (Fig. 2b).

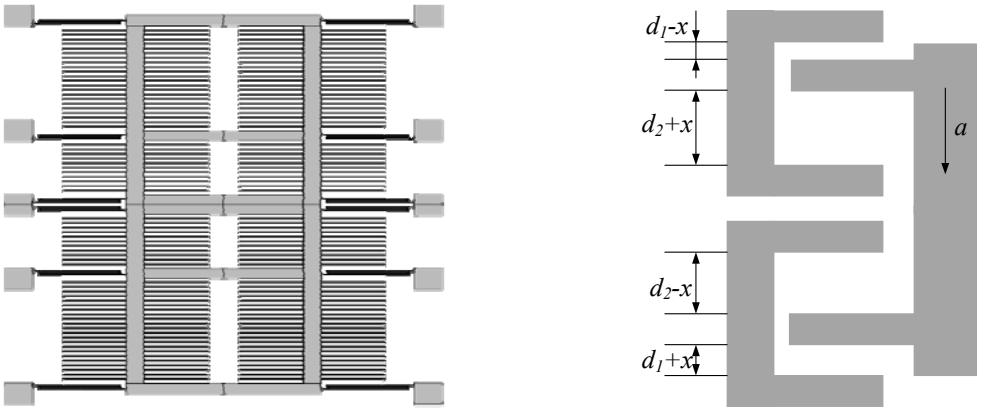


Fig. 2. Designed sensing element: a – mechanical (moving) part; b – principal scheme of gap-changing electrode structure.

Each electrode structure can be characterized by capacitance-voltage (C-V) characteristic, in particular, by capacitance variations due to the voltage on the electrodes, nominal electrode capacitance value (V = 0 V) and the differences between capacitances of differential electrode groups.

Packaging of SE with special IC and building MMA allow comparing SE-ELP with the purchased MMA SE. At this stage, we control the parameters in normal conditions, such as noise power density and nonlinearity, and within the entire temperature range (from minus 60 to plus 85 ºC), such as temperature variations of bias and scale factor.

To sum up, characterization of the SE-ELP consists of several steps:

- wafer-level testing that allows measuring directly the mechanical and electrical SE parameters;
- device-level testing that allows measuring parameters of the final device, i.e. the MMA.

The parameters determined at the first step can be used not only for proper chip selection for subsequent MMA fabrication, but also for preliminary IC trimming.

## 2. Wafer-level testing

Wafer level-testing makes it possible to directly estimate the electrical parameters of SE using special devices such as impedance analyzer, and to indirectly estimate the mechanical parameters using a sinusoidal oscillator to excite the proof-mass vibration on the resonance frequency [4]. However, the SE-ELP damping coefficient is very large, therefore, at the atmospheric pressure we can determine only electrical parameters.

### 2.1. Test equipment and methodology

The inspection system described in [4] is used for automatic control of the parameters of a wafer with more than 600 chips. It contains a semiconductor analyzer for C-V characteristic measurement, a

switch matrix for automatic commutations between different electrode groups, and a probe station for automatic precise movement from one chip to another during testing.

To control all these devices, the software was developed in LabView. The C-V characteristic measurement is organized by sweeping voltage $V$ on the electrodes and measuring their capacitance $C$. To measure the capacitance at each sweep step, the quasi-static capacitance measuring method is used [5]. The method is based on the measurements of the charge variation $\Delta Q$ caused by the voltage offset $\Delta V$ from the sweep step:

$$C = \frac{\Delta Q}{\Delta V} = \frac{\int idt}{\Delta V} \approx \frac{\sum i\Delta t,}{\Delta V}, \quad (1)$$

where $C$ is electrode capacitance, $i$ is current, $\Delta t$ is integration time, $\Delta V$ is voltage offset from the sweep step voltage.

Besides parameters measuring, the software provides compensation of the cable parasitic parameters to improve the accuracy of measurements.

## 2.2. Test results

The test results can be presented as a histogram to estimate the median value and the deviation of parameters, and as a yield map to estimate the distribution of a parameter on the wafer. The histograms for one of the detector electrode groups are shown in Fig. 3 (the results for other electrode groups are similar).

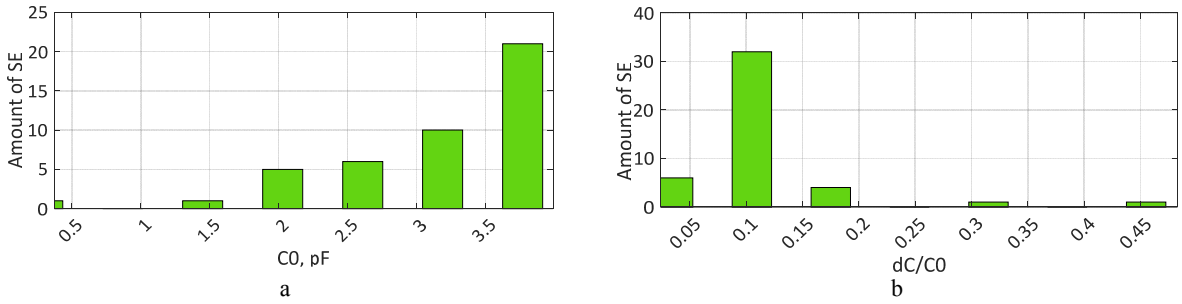


Fig. 3. Histograms for the first detector electrode group ED1: a – nominal capacitance; b – relationship of capacitance change (due to voltage) and nominal capacitance.

The test results with analytical parameter values calculated in course of design are summarized in Table 1.

T a b l e 1

**Results of wafer-level testing and analytical estimation**

| **Parameters** | **First detector electrode group (ED1)** | | **Second detector electrode group (ED2)** | | **First self-test electrode group (ES1)** | | **Second self-test electrode group (ES2)** | |
|---|---|---|---|---|---|---|---|---|
| | **$C_0$** | **dC/ $C_0$** | **$C_0$** | **dC/ $C_0$** | **$C_0$** | **dC/ $C_0$** | **$C_0$** | **dC/ $C_0$** |
| Analytical value, pF | 3.271 | 0.071 | 3.271 | 0.071 | 6.542 | 0.062 | 6.542 | 0.062 |
| Test value, pF | 3.434 | 0.099 | 3.447 | 0.095 | 6.749 | 0.071 | 6.736 | 0.085 |
| Difference, % | 4.730 | 28.28 | 5.090 | 25.26 | 3.060 | 12.67 | 2.870 | 27.06 |

The analysis of the test and analytical data shows that the measured median values of nominal electrode capacitance are close to the analytical ones (the difference between them is less than 5%). However, the measured values of the second parameter, the relationship of capacitance change (due to the voltage on electrodes) and nominal capacitance, differ from the analytical ones by 15-30%. To find the reasons of such an effect, we analyzed the following equations:

$$C_0 = \varepsilon\varepsilon_0 LhN\left(\frac{1}{d_1} + \frac{1}{d_2}\right), \quad (2)$$

$$dC / C_0 = \frac{\Delta C_V}{C_0} = \frac{\varepsilon\varepsilon_0 LhN\left(\frac{1}{d_1 - x_V} + \frac{1}{d_2 + x_V}\right) - C_0}{C_0}, \quad (3)$$

where $C_0$ is nominal electrode group capacitance; ε is permittivity; $\varepsilon_0$ is dielectric constant; $L$ is electrode overlap length; $h$ is electrode thickness; $d_1$, $d_2$ are the gaps between the electrodes; $N$ is electrode number, $\Delta C_V$ is capacitance change due to the voltage on the electrodes, and $x_V$ is electrode displacement due to voltage on the electrodes.

The formula of capacitance change differs from the formula of nominal capacitance by the component $x_V$ which is defined by the electrode geometrical parameters and by stiffness. Therefore, the values of difference between the analytical and test results mean that the effect of electrode overetching during fabrication process was taken into account, while the same effect for springs was ignored, and the resulting stiffness of all springs is smaller than designed. The value of difference around 30% means that the value of springs overetching is equal to 2.31 um:

$$\frac{k_1}{k_2} = \frac{N_s E h w_1^3}{L^3 N_f} \cdot \frac{L^3 N_f}{N_s E h w_2^3} = \frac{w_1^3}{w_2^3}, \quad (4)$$

where $k_1$ is the analytical value of stiffness; $k_2$ is the value of stiffness estimated from test results; $N_s$ is the number of springs; $E$ is Young's modulus; $h$ is spring thickness; $w_1$, $w_2$ are analytical and real values of spring width; $L$ is spring length; and $N_f$ is the number of folds in each spring.

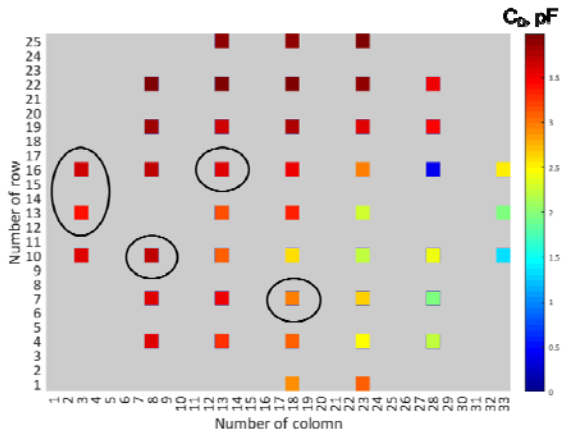


Fig. 4. Yield map for nominal capacitance of the first detector electrode group ED1.

The yield map (Fig.4) shows the spiral parameter scatter over the wafer, which results in the following median value of capacitance difference between a pair of electrodes:

- ED nominal capacitance difference: 0.012 pF;
- Difference of ED capacitance change due to voltage: 0.037 pF;
- ES nominal capacitance difference: 0.062 pF;
- Difference of ES capacitance change due to voltage: 0.134 pF.

The capacitance difference is not critical in normal conditions, because we can compensate it by IC trimming in the range from $10^{-3}$ pF to 13 pF; however, it can cause unsymmetrical thermal deformations leading to bias temperature variation of MMA in the whole temperature range.

## 3. Device-level testing

To analyze the influence of SE characteristics on MMA characteristics and to compare SE-ELP to a purchased MMA SE, six chips were selected according to the results of wafer-level testing (the selected chips are rounded with black circles in Fig.4). The criterion of selection is the minimal difference between nominal capacitances of detector electrodes group. These samples were packaged with IC which was a part of serial MMA and had low noise level around 50 zF/g and wide capacitance tuning range.

### 3.1. Test equipment and methodology

Thermal testing of the MMA was also organized with the use of automatic inspection system. The system consists of a rate table with a thermal chamber and a control computer that has two functions: controlling the equipment and collecting the data from sensors.

The test procedure consisted of two thermocycles. During one thermocycle, the temperature was changed from minus 60 to plus 85 ºC with a step of 15 ºC. At each temperature, the sensors were

exposed until the fluctuation of the sensor temperature was smaller than ±2 ºC for 20 minutes. After 20 minutes, the rotation stage consisting of 15 steps started. The acceleration acting on the sensors at each step was equal to the value of centripetal acceleration, as the sensors were installed at some distance from the axis of rotation:

$$a_i = \omega_i^2 R, \tag{5}$$

where $a_i$ is acceleration acting on the sensors at each step; $\omega_i$ is the angular velocity at each step, $R$ is the distance from the SE mass center to the axis of rotation.

To estimate the value of nonlinearity, the MMA data at the temperature of 25 ºC were used. The methodology of noise power density estimation is presented in [6].

### 3.2. Test results

The noise power density values for serial MMA and for MMA with SE-ELP are 36 ug/√Hz and 22.5 ug/√Hz, respectively. Despite the greatest contribution of IC noise level to the device noise level, the lower noise level for our sensor is determined by the mechanical noise of the SE, equal to 3.06 ug/√Hz, whereas the mechanical noise of the purchased SE is 13.2 ug/√Hz.

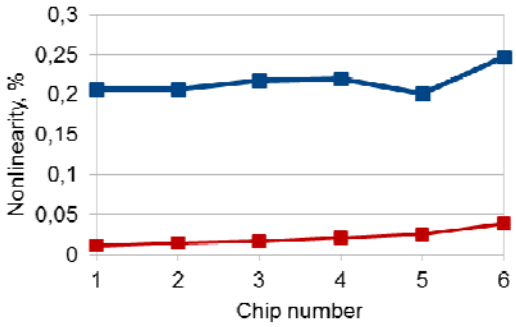


Fig. 5. Nonlinearity of MMA (red line: MMA with purchased SE; blue line: MMA with SE-ELP).

The results for another characteristic, i.e. nonlinearity, estimated in normal conditions are shown in Fig. 5. This characteristic, as well as the thermal characteristics described below are shown in comparison with the serial sensor. For every characteristic, a batch of 100 serial sensors was streamlined from the minimum to the maximum characteristic values, and divided into six groups. Then the mean value of characteristic in each group was plotted. The MMA with SE-ELP worked in the open-loop mode, so its nonlinearity defined by nonlinearity of the gap changing electrode structure is twice larger than the serial one has. The next step of our work will be SE-ELP bonding with IC in the close-loop mode and using the self-test electrodes as actuators to decrease the nonlinearity of the sensor.

Temperature errors after calibration with the 4th degree polynomial are given in Fig. 6. The scale factor temperature variation in the MMA with SE-ELP is at the same level as in the best ones among the serial MMA. The bias temperature variation is at the level of medium ones among the serial MMA.

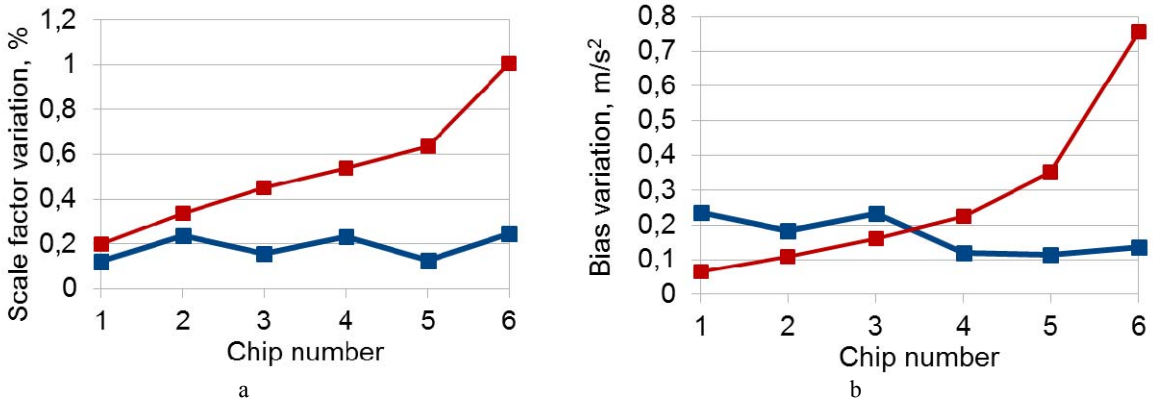


Fig. 6. MMA thermal characteristics: a – scale factor temperature variation; b – bias temperature variation (red line: MMA with purchased SE; blue line: MMA with SE-ELP).

In order to substantiate these results, additional modeling of the SE behavior in the whole temperature range and estimation of the thermal deformation values are required. Moreover, it is necessary to conduct additional wafer-level tests with evaluation of SE parameters dependence on temperature changes.

Based on the above, it can be noted that the SE-ELP has the characteristics that are none the worse than those of the purchased SE; thus, our SE can be used in MMA production.

## Conclusions

Wafer-level and device-level testing for SE-ELP, the sensing element of the capacitive MMA designed at Concern CSRI Elektropribor, JSC, have been described in terms of the test procedures and results. During wafer-level testing, the electrical parameters of the manufactured SE were controlled and compared to the analytical ones. Distribution of the parameters over the wafer has been estimated. This analysis helped to determine the influence of the technological error on the SE parameters. The measured parameter variations should be included in mathematical models and taken into account for topology corrections.

During device-level testing, the MMA based on SE-ELP and on the purchased SE have been characterized and compared. According to the results, the SE-ELP can be used in MMA production. The analysis of the test results has shown that it is necessary to increase the amount of wafer-level controlled parameters by adding temperature variations.

REFERENCES

[1] Peshekhonov, V.G., Gyroscopic navigation systems: current status and prospects, Gyroscopy and Navigation, 2011, no. 3, pp. 111–118.
[2] Belyaev, Ya.V., Belogurov, A.A., Kostygov, D.V., Lemko, I.V., Mihteeva, A.A., Yakimova, A.V., Nevirkovets, N.N. and Chernetskaya, N.M., Design of a micromechanical accelerometer, Proc. 25th Saint Petersburg International Conference on Integrated Navigation Systems, Saint Petersburg, 2018.
[3] Yakimova, A.V., Belogurov, A.A. and Belyaev, Y.V., Design of sensing element of micromachined capacitive MEMS accelerometer, Proc. International Workshop “Navigation and Motion Control”, 2017.
[4] Yakimova, A.V., Belogurov, A.A. and Belyaev, Y.V., Input control arrangement for sensing elements of wafer-based micromechanical sensors , Datchiki i sistemy, 2017, no. 2, pp. 47–52.
[5] Wadsworth, A., The Parametric Measurement Handbook, Keysight Technologies, 2017.
[6] IEEE standard Specification Format Guide and Test Procedure for Linear Single-Axis, Nongyroscopic Accelerometers.